ChemComm

COMMUNICATION

View Article Online
View Journal | View Issue

A novel CO_2-stable dual phase membrane with high oxygen permeability†

Cite this: *Chem. Commun.*, 2014, 50, 2451

Received 16th October 2013,
Accepted 9th January 2014

DOI: 10.1039/c3cc47962e

www.rsc.org/chemcomm

Fangyi Liang,*[a] Huixia Luo,[b] Kaveh Partovi,[a] Olga Ravkina,[a] Zhengwen Cao,[a] Yi Liu[a] and Jürgen Caro[a]

By cobalt-doping of the mixed conducting phase PSFC, a good combination of high CO_2 stability and high oxygen permeability is obtained for the 60 wt% $Ce_{0.9}Pr_{0.1}O_{2-\delta}$–40 wt% $Pr_{0.6}Sr_{0.4}Fe_{0.5}Co_{0.5}O_{3-\delta}$ (CP–PSFC) dual phase membrane, which suggests that CP–PSFC is a promising membrane for industrial applications in the oxyfuel process for CO_2 capture.

CO_2 capture and storage technologies in power plants have gained attention worldwide[1] since the combustion of fossil fuel is considered to be the main contribution to CO_2 emissions. Oxygen transporting membranes (OTMs)[2] based on mixed electronic and ionic conductors, can supply oxygen of 100% purity to power stations for CO_2 capture according to the oxyfuel for CO_2 capture and storage.[3] The oxyfuel concept involves the combustion of fossil fuels with an oxygen/exhaust gas mixture. The pure oxygen used in the oxyfuel process can be produced using the Linde cryogenic technique. However, by using OTMs, oxygen can be separated from air by using a part of the exhaust gas CO_2 as a sweep gas. Oxygen production by using OTMs can reduce the costs by 35% and save 60% energy compared to the conventional cryogenic process.[4] A part of the exhaust gas CO_2 is sequestrated, and another part is recycled and used as sweep gas for the oxygen separation through the OTMs. Thus, the OTMs for CO_2 capture in the oxyfuel process should have not only good stability in a CO_2 atmosphere but also high oxygen permeation performance at elevated temperatures. Moreover, OTMs can be used in many promising potential applications, such as in high-purity oxygen production,[5] in catalytic membrane reactors,[6] and as cathodes in solid oxide fuel cells (SOFCs).[7]

Among OTMs, many cobalt-based single phase perovskite-type membranes such as $Ba_{1-x}Sr_xCo_{1-y}Fe_yO_{3-\delta}$ exhibit high oxygen permeability[8] since cobalt can provide a high concentration of mobile oxygen vacancies in the perovskite lattice over a wide temperature range.[9] However, under a CO_2 atmosphere these membranes immediately lose their oxygen permeation flux, since the alkaline-earth metals on the A site of the perovskite framework form carbonates with CO_2.[10] Recently, dual phase membranes with good structural stability and CO_2 resistance, made of a micro-scale mixture of well separated grains of the two phases of an oxygen ionic conductor and an electronic conductor, have attracted much attention for the application of the O_2 production in the oxyfuel concept. However, the low oxygen permeability of dual phase membranes needs to be improved to meet the industrial application requirements.[11] Zhu *et al.* improved the oxygen permeability of their CO_2-stable dual phase membranes, such as $Ce_{0.8}Sm_{0.2}O_{1.9}$–$SmMn_{0.5}Co_{0.5}O_3$[12] and $Ce_{0.85}Sm_{0.15}O_{1.925}$–$Sm_{0.6}Sr_{0.4}FeO_3$,[13] by coating Co-containing porous layers on the membrane surface to enlarge the oxygen exchange surface. In our group, we have developed some novel Co-free CO_2-stable dual phase membranes, such as $NiFe_2O_4$–$Ce_{0.9}Gd_{0.1}O_{2-\delta}$ (NF–CG),[14] Fe_2O_3–$Ce_{0.9}Gd_{0.1}O_{2-\delta}$ (F–CG)[15] and $Ce_{0.9}Pr_{0.1}O_{2-\delta}$–$Pr_{0.6}Sr_{0.4}FeO_{3-\delta}$ (CP–PSF).[16] The CP–PSF membrane shows a good chemical stability under the harsh conditions of the POM reaction and in a CO_2 atmosphere at high temperatures.[16] Thus, cobalt-doping of the PSF phase in the dual phase CP–PSF membrane can enhance the oxygen vacancy concentration in the membrane lattice, which should result in a combination of good CO_2 stability and high oxygen permeability.

In this paper, we present the novel dual phase membrane, 60 wt% $Ce_{0.9}Pr_{0.1}O_{2-\delta}$–40 wt% $Pr_{0.6}Sr_{0.4}Fe_{0.5}Co_{0.5}O_{3-\delta}$ (abbreviated as CP–PSFC) prepared *via* a one-pot sol–gel synthesis method.[17] In this dual phase system, the CP phase is mainly for ionic transport, and the PSFC phase for both electronic and ionic transport. The XRD pattern in Fig. 1 shows that after sintering at 1200 °C for 5 h in air, the dual phase CP–PSFC membrane consists of only the cubic flourite CP phase (space group 225: *Fm3m*) and the orthorhombic distorted perovskite PSFC phase (space group 74: *Imma*). The phase stability of the dual phase CP–PSFC material against CO_2 was evaluated by *in situ* XRD measurements (Fig. S2, ESI†) between 30 and 1000 °C in an atmosphere of 50 vol% CO_2/50 vol% air. No carbonate formation was observed in the *in situ* XRD patterns

[a] *Institute of Physical Chemistry and Electrochemistry, Leibniz University of Hannover, Callinstr. 3a, D-30167 Hannover, Germany. E-mail: fangyi.liang@pci.uni-hannover.de; Fax: +49-511-762-19121; Tel: +49-511-762-2942*

[b] *Department of Chemistry, Princeton University, Princeton, New Jersey 08544, USA*

† Electronic supplementary information (ESI) available: Experimental details. See DOI: 10.1039/c3cc47962e

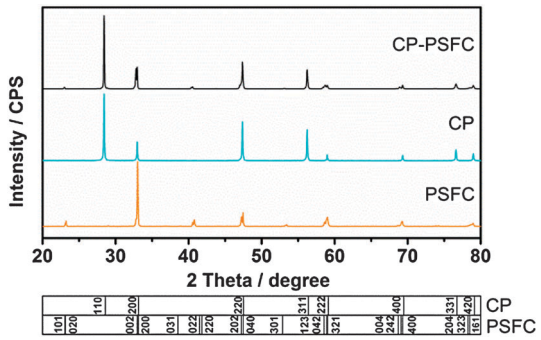

Fig. 1 XRD patterns of the dual phase CP–PSFC membrane, and of the single phases CP and PSFC, all sintered at 1200 °C in air for 5 h.

from 30 to 1000 °C, which is in good agreement with the *in situ* XRD finding in previous reports of the CP–PSF[16] and $La_{0.6}Sr_{0.4}Co_{0.8}Fe_{0.2}O_{3-\delta}$[18] under similar experimental conditions. In this temperature range, the CP phase retains the cubic structure. Moreover, two phase transitions of the PSFC phase from the orthorhombic to the rhombohedral symmetry at *ca.* 600 °C and from the rhombohedral to the cubic symmetry at *ca.* 800 °C could be observed. However, the PSF phase without Co in the dual phase CP–PSF powder retains the orthorhombic symmetry under the same conditions.[16] The phase transition from rhombohedral to cubic symmetry at high temperatures is in agreement with the findings for the comparable materials $La_{0.6}Sr_{0.4}Co_{0.8}Fe_{0.2}O_{3-\delta}$[18] and $La_{0.6}Ca_{0.4}Co_{0.8}Fe_{0.2}O_{3-\delta}$.[19] The formation of the cubic structure of the PSFC phase at high temperatures is beneficial for oxygen permeability.[17,20] Thus, the dual phase CP–PSFC material exhibits a stable co-existence of both the CP and the PSFC phases and a good tolerance against CO_2.

Fig. 2 shows the scanning electron microscopy (SEM), backscattered SEM (BSEM), and energy-dispersive X-ray spectroscopy (EDXS) images of the dual phase CP–PSFC membrane after sintering at 1200 °C for 5 h in air. SEM (Fig. 2a) indicates that the membrane is dense. In the BSEM (Fig. 2b and c) at different magnifications, the grains of the two phases are well distributed forming a 3-dimensional percolation network with clear grain boundaries, which is beneficial to the oxygen ion and electron transport through the membrane. The light grains in the BSEM are CP and the dark grains are PSFC since the contribution of the backscattered electrons to the SEM signal intensity is proportional to the atomic number. The grain size of CP in these composite membranes is larger than that of PSFC. The same information about the phase distribution is provided by the EDXS (Fig. 2d–f) of the membrane. Fig. 2d shows the color version EDXS of the membrane where the turquoise color (light in BSEM) is due to overlapping of the Ce and Pr signals, whereas the orange color (dark in BSEM) stems from an average of the Pr, Sr, Fe and Co signals. The EDXS elemental distributions of Ce in the CP grains (Fig. 2e) and of Sr in the PSFC grains (Fig. 2f) indicate the phase separation in the membrane and proof that no intermixing of Ce and Sr between the two phases exists.

The oxygen permeation fluxes through the dual phase CP–PSFC membrane as a function of temperature with pure He and CO_2 as sweep gases are shown in Fig. 3. For both the sweep gases He and CO_2, the oxygen permeation flux increases with increasing temperatures. By increasing the temperatures from 800 to 1000 °C, the oxygen permeation fluxes increase from 0.24 to 1.08 cm^3 (STP) min^{-1} cm^{-2} for using He and from 0.11 to 1.01 cm^3 (STP) min^{-1} cm^{-2} for using CO_2 as the sweep gas. If pure CO_2 has been used as the sweep gas, the oxygen permeation flux is only slightly lower than in the case when pure He was used as the sweep gas, which is in good agreement with the observations in previous reports.[13,14,21] The reason for this experimental finding can be attributed to the weaker adsorptive interaction of He in comparison with CO_2 with the membrane surface, as the influence of He on the oxygen exchange reaction is less than that of CO_2.[12,14,22,23] Furthermore, it is also found that the difference in the oxygen permeation flux between He and CO_2 as sweep gases is larger at lower temperatures and becomes smaller at higher temperatures, which can be ascribed to the decreasing adsorptive interaction with increasing temperatures. In comparison with the Co-free dual phase CP–PSF membrane at 950 and 1000 °C,[16] the oxygen permeation fluxes of the Co-containing dual phase CP–PSFC membrane are increased by approximately a factor of 3, which is a clear indication of an increased concentration of mobile oxygen vacancies by Co-doping, which significantly enhances the oxygen permeability of the PSFC phase.

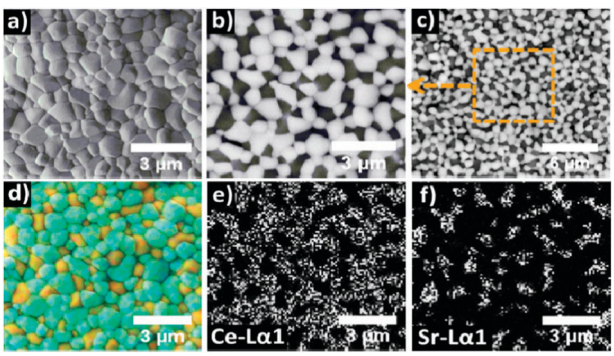

Fig. 2 SEM (a), BSEM (b and c), and EDXS (d–f) images of the dual phase CP–PSFC membrane after sintered at 1200 °C for 5 h in air. In BSEM (b and c) for different magnifications, the dark grains represent PSFC, the light ones CP. Superimpositions of the Pr, Sr, Fe and Co (orange), and Pr and Ce (turquoise) signals have been used in Fig. 2(d). Element distribution of Ce in the CP grains (Fig. 2e) and Sr in the PSFC (Fig. 2f).

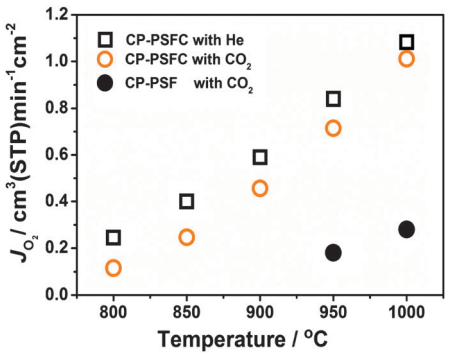

Fig. 3 Oxygen permeation fluxes through the dual phase CP–PSFC and CP–PSF[25] membranes as a function of temperature with pure He and CO_2 as sweep gases. Conditions for CP–PSFC: 150 cm^3 (STP) min^{-1} air as the feed gas, 50 cm^3 (STP) min^{-1} He or CO_2 as the sweep gas; membrane thickness: 0.6 mm. Conditions for CP–PSF:[16] 150 cm^3 (STP) min^{-1} air as the feed gas, 30 cm^3 (STP) min^{-1} CO_2 as the sweep gas; membrane thickness: 0.5 mm.

The oxygen permeability of an OTM strongly depends on its composition, the membrane thickness, the coating of the membrane surface (catalytic coating or coating to enlarge the surface, thus enhancing the exchange reaction), and the operation conditions (type of sweep gas, temperature, or the oxygen partial pressure). Table S1 (ESI†) contains the oxygen permeation fluxes of several OTMs evaluated with CO_2 as the sweep gas at *ca.* 950 °C. As shown in Table S1 (ESI†), our dual phase CP–PSFC membrane exhibits the highest oxygen permeation flux compared to the other dual phase membranes. It should be noted that the fluxes measured on our dual phase CP–PSFC membrane were obtained for a relatively thick membrane (0.6 mm) without any coating on the membrane surface. It is believed that the oxygen permeability of our CP–PSFC membrane can be further improved by reducing the membrane thickness like a hollow fiber membrane[23,24] or an asymmetric membrane,[25] or by coating for an enlargement of the membrane surface.[12,13]

Fig. 4 presents the long-term oxygen permeation operation of two dual phase CP–PSFC membranes M1 and M2. For the CP–PSFC membrane M1, when He is used as the sweep gas at 950 °C, the oxygen permeation flux increases slowly during the activation time in the first 10 h. After this activation step, the oxygen permeation flux reaches steady-state with a constant value of 0.84 cm^3 (STP) min^{-1} cm^{-2} (inset in Fig. 4). When pure CO_2 was used instead of He as the sweep gas, the oxygen permeation flux only slightly decreased to the lower value of 0.70 cm^3 (STP) min^{-1} cm^{-2}. This oxygen permeation flux was found to be constant during the whole oxygen permeation operation by using pure CO_2 as the sweep gas at 950 °C for 400 h. When the operation temperature was elevated to 1000 °C, the oxygen permeation flux increased significantly to the higher value of 1.01 cm^3 (STP) min^{-1} cm^{-2} and was constant for at least 100 h. Whereas the CP–PSFC membrane M1 shows a phase transition from the rhombohedral to the cubic phase (Fig. S2, ESI†) and a fast activation step over 10 h only at the higher temperature of 950 °C, when cooling the CP–PSFC membrane M2 from 950 to 800 °C, a phase transition from the cubic to the orthorhombic phase takes place (Fig. S2, ESI†). After this phase transition, a slow activation step takes place over *ca.* 100 h at the lower temperature of 800 °C. As a result of (i) the phase transformation, and (ii) the lower permeation temperature, for the CP–PSFC membrane M2 with pure CO_2 as the sweep gas at 800 °C, the oxygen permeation flux decreases slowly from 0.19 to 0.13 cm^3 (STP) min^{-1} cm^{-2} in the first 100 h. After this phase transformation and the activation step, the oxygen permeation flux reaches a steady-state for 200 h. For the membranes M1 and M2 after the long-term oxygen permeation operation, no carbonate formation was observed in the XRD patterns (Fig. S3 and S5, ESI†). No carbon species enrichment was found at the strontium positions in the EDXS images on the surfaces of the membranes M1 and M2 (Fig. S6 and S7, ESI†) and their cross-sections (Fig. S4 and S8, ESI†), which excludes $SrCO_3$ formation. This long-term operations suggest that our dual phase CP–PSFC membrane exhibits an excellent stability in CO_2 and shows a high oxygen permeation performance.

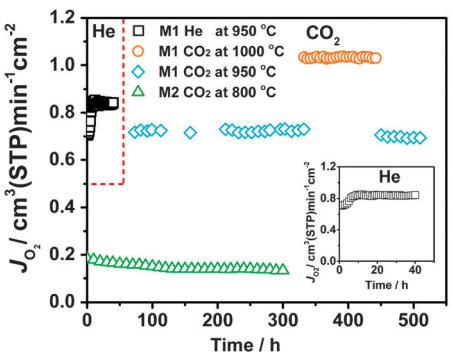

Fig. 4 Long-term oxygen permeation operation of two dual phase CP–PSFC membranes M1 and M2 with pure He or CO_2 as sweep gases at different temperatures. The inset magnifies the oxygen permeation operation with pure He as the sweep gas at 950 °C. Conditions: 150 cm^3 min^{-1} air as the feed gas, 50 cm^3 min^{-1} He or CO_2 as the sweep gas; membrane thickness: 0.6 mm.

In summary, we have prepared a novel CO_2-stable dual phase 60 wt% $Ce_{0.9}Pr_{0.1}O_{2-\delta}$–40 wt% $Pr_{0.6}Sr_{0.4}Fe_{0.5}Co_{0.5}O_{3-\delta}$ (CP–PSFC) membrane with Co-doping of the PSF phase for high oxygen permeability. Cobalt-doping of the PSF phase can enhance the oxygen vacancy concentration in the membrane lattice and stabilize the cubic structure above 800 °C which is beneficial for oxygen permeability. The *in situ* XRD and the long-term operations demonstrate that the CP–PSFC dual phase membrane shows a very good tolerance against CO_2. Moreover, the very high oxygen permeation flux of 0.70 and 1.01 cm^3 (STP) min^{-1} cm^{-2} were found to be constant at 950 and 1000 °C during the long-term operation for over at least 400 h. The dual phase CP–PSFC membrane with excellent CO_2 stability and high oxygen permeation performance is a promising membrane material for industrial applications in the oxyfuel process for CO_2 capture.

The EU is thanked for financing the 7th Framework Program of the IP Innovative Catalytic Technologies & Materials for the Next Gas to Liquid Processes (NEXT-GTL). The authors are thankful for the financial support by DFG 147/18-1 and to the Sino-German Center for Promoting Research (GZ 676). The authors thank Prof. Dr Feldhoff for stimulating discussions and F. Steinbach for technical support.

Notes and references

1 R. S. Haszeldine, *Science*, 2009, **325**, 1647–1652.
2 S. P. S. Badwal and F. T. Ciacchi, *Adv. Mater.*, 2001, **13**, 993–996; Y. Y. Liu, X. Y. Tan and K. Li, *Catal. Rev.: Sci. Eng.*, 2006, **48**, 145–198; J. Sunarso, S. Baumann, J. M. Serra, W. A. Meulenberg, S. Liu, Y. S. Lin and J. C. D. da Costa, *J. Membr. Sci.*, 2008, **320**, 13–41.
3 A. Leo, S. Liu and J. C. D. da Costa, *Int. J. Greenhouse Gas Control*, 2009, **3**, 357–367; X. Y. Tan, K. Li, A. Thursfield and I. S. Metcalfe, *Catal. Today*, 2008, **131**, 292–304.
4 P. A. Armstrong, D. L. Bennett, E. P. T. Foster and E. E. van Stein, *ITM oxygen for gasification, Proceedings of Gasification Technologies Conference*, Washington, DC, USA, 2004.
5 X. F. Zhu, S. M. Sun, Y. Cong and W. S. Yang, *J. Membr. Sci.*, 2009, **345**, 47–52; F. Y. Liang, H. Q. Jiang, T. Schiestel and J. Caro, *Ind. Eng. Chem. Res.*, 2010, **49**, 9377–9384; F. Y. Liang, H. Q. Jiang, H. X. Luo, R. Kriegel and J. Caro, *Catal. Today*, 2012, **193**, 95–100.
6 H. Q. Jiang, H. H. Wang, F. Y. Liang, S. Werth, T. Schiestel and J. Caro, *Angew. Chem., Int. Ed.*, 2009, **48**, 2983–2986; Y. Y. Wei, W. S. Yang, J. Caro and H. H. Wang, *Chem. Eng. J.*, 2013, **220**, 185–203.
7 Z. P. Shao and S. M. Haile, *Nature*, 2004, **431**, 170–173.
8 Z. P. Shao, W. S. Yang, Y. Cong, H. Dong, J. H. Tong and G. X. Xiong, *J. Membr. Sci.*, 2000, **172**, 177–188; J. F. Vente, S. McIntosh, W. G. Haije and H. J. M. Bouwmeester, *J. Solid State Electrochem.*, 2006, **10**, 581–588.

9 R. Kriegel, R. Kircheisen and J. Töpfer, *Solid State Ionics*, 2010, **181**, 64–70.
10 M. Arnold, H. H. Wang and A. Feldhoff, *J. Membr. Sci.*, 2007, **293**, 44–52; A. Waindich, A. Möbius and M. Müller, *J. Membr. Sci.*, 2009, **337**, 182–187; S. Engels, F. Beggel, M. Modigell and H. Stadler, *J. Membr. Sci.*, 2010, **359**, 93–101.
11 B. C. H. Steele, *Curr. Opin. Solid State Mater. Sci.*, 1996, **1**, 684–691.
12 X. F. Zhu, H. Y. Liu, Y. Cong and W. S. Yang, *Chem. Commun.*, 2012, **48**, 251–253.
13 X. F. Zhu, M. R. Li, H. Liu, T. Y. Zhang, Y. Cong and W. S. Yang, *J. Membr. Sci.*, 2012, **394**, 120–130.
14 H. X. Luo, K. Efimov, H. Q. Jiang, A. Feldhoff, H. H. Wang and J. Caro, *Angew. Chem., Int. Ed.*, 2011, **50**, 759–763.
15 H. X. Luo, H. Q. Jiang, K. Efimov, F. Y. Liang, H. H. Wang and J. Caro, *Ind. Eng. Chem. Res.*, 2011, **50**, 13508–13517.
16 H. X. Luo, H. Q. Jiang, T. Klande, Z. W. Cao, F. Liang, H. H. Wang and J. Caro, *Chem. Mater.*, 2012, **24**, 2148–2154.
17 F. Y. Liang, K. Partovi, H. Q. Jiang, H. X. Luo and J. Caro, *J. Mater. Chem. A*, 2013, **1**, 746–751.
18 T. Klande, O. Ravkina and A. Feldhoff, *J. Membr. Sci.*, 2013, **437**, 122–130.
19 K. Efimov, T. Klande, N. Juditzki and A. Feldhoff, *J. Membr. Sci.*, 2012, **389**, 205–215.
20 X. T. Liu, H. L. Zhao, J. Y. Yang, Y. Li, T. Chen, X. G. Lu, W. Z. Ding and F. S. Li, *J. Membr. Sci.*, 2011, **383**, 235–240; X. F. Zhu, H. H. Wang and W. S. Yang, *Chem. Commun.*, 2004, 1130–1131.
21 H. X. Luo, H. Q. Jiang, T. Klande, F. Y. Liang, Z. W. Cao, H. H. Wang and J. Caro, *J. Membr. Sci.*, 2012, **423**, 450–458.
22 S. M. Fang, C. S. Chen and L. Winnubst, *Solid State Ionics*, 2011, **190**, 46–52; J. E. tenElshof, H. J. M. Bouwmeester and H. Verweij, *Solid State Ionics*, 1996, **89**, 81–92.
23 W. Li, T. F. Tian, F. Y. Shi, Y. S. Wang and C. S. Chen, *Ind. Eng. Chem. Res.*, 2009, **48**, 5789–5793.
24 W. Li, J. J. Liu and C. S. Chen, *J. Membr. Sci.*, 2009, **340**, 266–271.
25 S. Baumann, J. M. Serra, M. P. Lobera, S. Escolastico, F. Schulze-Kueppers and W. A. Meulenberg, *J. Membr. Sci.*, 2011, **377**, 198–205; M. P. Lobera, J. M. Serra, S. P. Foghmoes, M. Sogaard and A. Kaiser, *J. Membr. Sci.*, 2011, **385**, 154–161.

